A simple 3D susceptibility model to simulate magnetic field patterns in white matter microstructure

W. Chen[1], and K. L. Miller[1]
[1]FMRIB, University of Oxford, Oxford, Oxon, United Kingdom

Introduction. Recent studies of susceptibility-weighted imaging (GRE phase and magnitude) have revealed significant heterogeneity in white matter, which appears to relate in part to the orientation of fiber tracts to B0 [1-4]. Several studies have proposed sources for this orientation dependence, including susceptibility anisotropy from membrane phospholipids [2] and susceptibility "inclusions" associated with axons [3]. However, these studies have not explicitly modeled the separate micro-structural compartments, but based their calculations on a weighted mean susceptibility. An alternative approach to modeling the origins of the signal properties in white matter is to build a digital phantom of tissue microstructure compartments. Our model generates a 3D "voxel" containing susceptibility-shifted cylinders and spheres and calculates the resulting field patterns.

Methods. Our 3D voxel contains 3 micro-structural compartments: extracellular space, axons and oligodendrocytes (glia) (see Fig 1e). Axons are modeled as concentric cylinders with a myelin layer and cytoplasm. Oligodendrocytes are modeled as solid spheres. The axons are first arranged in a hexagonal pattern with a pre-defined radius distribution and volume fraction. The oligodendrocytes are then randomly superimposed onto the same volume of interest with a pre-defined concentration. Susceptibility values for each compartment are taken from existing literature. Susceptibility anisotropy is introduced in the myelin compartment [3]. The susceptibility value of each compartment is slightly varied across cells to make the susceptibility distribution more realistic. The 3D Fourier method was then used to calculate the field pattern resulting from the susceptibility map [1]. In this abstract, two models were tested, they are: (1) myelinated axons only and (2) myelinated axons and oligodendrocytes. Field patterns were generated with B0 parallel (see Fig 1b/f) and perpendicular (see Fig 1c/g) to the long axis of the axon. Mean radii of cellular compartments were: axon inner=0.7um, myelin outer=1um, oligodendrocyte=4um [10], with random perturbations of 10% about the mean. The concentration of oligodendrocytes was taken to be 125000/mm^2 [8]. The size of the total simulation matrix is 800x800x800 over 5.12 x 10^{-4} mm^3. Intracellular volume was maintained at approximately 70% of the whole volume. The extracellular fluid was assumed to have the susceptibility value of water, which was used as the reference frequency. The susceptibility value of myelin was set at -0.180 ppm when parallel to B0 and -0.192ppm when perpendicular to B0 [3]. Assuming that most iron-bounded ferritin molecules are evenly distributed in the oligodendrocyte, the susceptibility of oligodendrocytes was calculated from 1.4ppm/mg Fe/g tissue and 0.04mg ferritin/g tissue [7]. The susceptibility value of the intra-axonal space was then set such that the overall susceptibility is 0.05 ppm.

Results and discussions. One goal of this work is to derive measures (see Table 1) that can be compared with literature values. The model without oligodendrocytes predicted a larger positive mean frequency for the perpendicular direction (consistent with literature), which reversed when oligodendrocytes were included (not consistent). In general, however, our present model was found to be unstable with respect to estimating the mean frequency. This appears to result from the regular (hexagonal) axonal packing, which causes the mean to depend strongly on the precise cutoff of the voxel edges. Future work will simulate more biologically-plausible axon packing patterns, which requires sophisticated algorithms to achieve large intracellular fractions. The standard deviations obtained from both models were found to be in approximate agreement with reported T2* values [6,9]. In addition, our model provides a means of studying the entire frequency distribution of the susceptibility model (see Fig 1d/h). GRE measurements of phase and magnitude reflect the distribution mean and variance, respectively. Our simulations indicate that other distribution properties could be a rich source of information if techniques that are sensitive to these properties can be developed [5,6]. For example, of the values reported in Table 1, the skew is arguably the most affected by the inclusion of oligodendrocytes. One difficulty in this kind of modeling is the paucity of literature on susceptibility values for the tissue constituents of interest. Also, it should be noted that our simulated 'voxel' is much smaller than a typical imaging voxel (~1mm^3). Future work will simulate more realistic voxel sizes and the effects of diffusion, both requiring careful optimization due to increased computational burden. Ultimately, we hope to use this model to predict changes in frequency distribution due to changes in the white matter microstructure during diseases e.g. thinning of myelin sheaths and increased iron concentration.

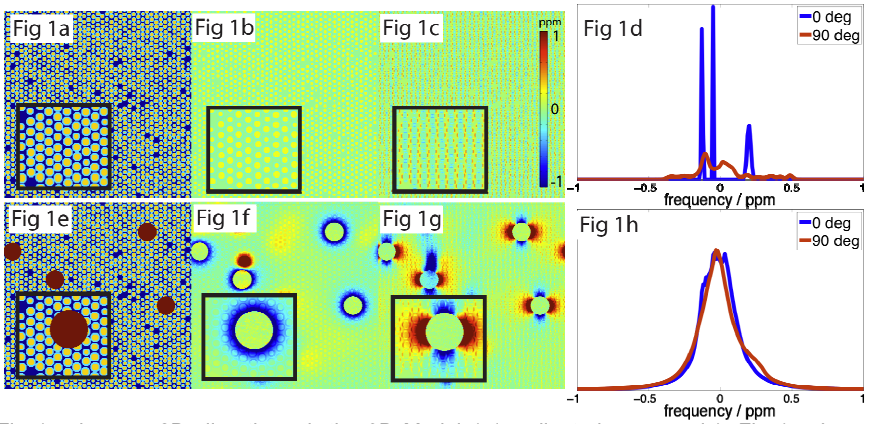

Fig 1a shows a 2D slice through the 3D Model 1 (myelinated axons only). Fig 1e shows the 3D Model 2 (myelinated axons and oligodendrocytes). Red = oligodendrocyte, Yellow = axon, Dark Blue = extracellular fluid, Light Blue = myelin. Each fiber has a radius of approximately 1um. The box at the bottom left is a zoom-in section. The frequency map generated at 0 degrees and 90 degrees to B0 are shown in Fig 1b/f and 1c/g respectively. The histograms of the frequency maps are shown in Fig 1d/h.

	Without oligodendrocyte		With oligodendrocyte	
	0 deg	90 deg	0 deg	90 deg
Mean	-7.85 ±0.53	15.09 ±0.57	11.58 ±0. 24	-0.83 ± 0.17
Stdev	0.139 ±0.000	0.182 ±0.000	0.281 ±0.002	0.292 ±0.002
Skew	.254 ±0.002	0.555 ±0.006	5.087 ±0.759	4.822 ±0.650

Table 1: measured moments of frequency distribution (ppm except mean in 10^{-4}ppm)

References: [1] Marques, NeuroIm 2009. [2] He, PNAS 2009. [3] Lee, PNAS 2010. [4] Liu, MRM 2010. [5] Al-Hallaq, NMRBiom 2002. [6] Miller MRM 2010. [7] Duyn, PNAS 2007. [8] Segal, ActaNeuro 2009. [9] Peters, MRM 2007. [10] Kettenmann, Neuroglia 2005.